Urban land-cover classification based on airborne hyperspectral data and field observation

Fumio Yamazaki*[a], Konomi Hara[a], Wen Liu[a]
[a] Graduate School of Eng., Chiba University, 1-33 Yayoi-cho, Inage-ku, Chiba, Japan 263-8522

ABSTRACT

Using a dataset from the 2013 IEEE data fusion contest, a basic study to classify urban land-cover was carried out. The spectral reflectance characteristics of surface materials were investigated from the airborne hyperspectral (HS) data acquired by CASI-1500 imager over Houston, Texas, USA. The HS data include 144 spectral bands in the visible to near-infrared (380 nm to 1050 nm) regions. A multispectral (MS) image acquired by WorldView-2 satellite was also introduced in order to compare it with the HS image. A field measurement in the Houston's test site was carried out using a handheld spectroradiometer by the present authors. The reflectance of surface materials obtained by the measurement was also compared with the pseudo-reflectance of the HS data and they showed good agreement. Finally a principal component analysis was conducted for the HS and MS data and the result was discussed.

Keywords: hyperspectral data, CASI-1500, WorldView-2, spectroradiometer, reflectance

1. INTRODUCTION

Recent advancements of remote sensing technology have enabled fine identification of surface materials due to improved spatial, temporal and spectral resolutions of sensors. The improvement in spatial resolution of satellite optical sensors is most drastic and the resultant very high-resolution images are now widely available through Google Earth. Fine spatial-resolution also helps to identify detailed damage situation of urban areas due to natural disasters, e.g. earthquakes and hurricanes [1-4].

Urban environment is generally complicated, mixture of both natural land-cover (e.g. bare ground, water, vegetation) and man-made or impervious land-cover (e.g. roads, buildings). The distribution of land-cover classes is important for environmental management, disaster management and urban planning. There have been many researches focusing on the classification of vegetation in agricultural lands or forests. However, researches on the classification of man-made land-surfaces in urban areas are still limited due to their high complexity. Owing to the fine spectral resolution, hyperspectral remote sensing data have potential to classify artificial land-cover with different materials. Hyperspectral remote sensing technology has advanced significantly in the last few decades and its overview is provided in literature [5, 6]. Several airborne and spaceborne instruments with over 200 spectral bands have already been developed and actually in use. Since hyperspectral imaging provides many narrow-banded images simultaneously, the acquired data should be compared with the spectral reflectance characteristics of surface materials from spectral library or by field observation [7].

In this study, a basic study to classify urban land-cover and land-use was carried out using a dataset from the 2013 IEEE data fusion contest [8]. Firstly, the spectral characteristics for both natural surfaces and artificial structures are investigated using the airborne hyperspectral data covering a part of Houston, Texas, USA, and they are compared with the ground-based spectral observation results, conducted in Houston, Texas by the present authors. A principal component analysis (PCA) is carried out for the hyperspectral data and an 8-band WorldView-2 image covering the same area and their results are compared.

2. THE STUDY AREA AND IMAGERY DATA USED

The Data Fusion Technical Committee of the IEEE Geoscience and Remote Sensing Society (GRSS) conducts Data Fusion Contest in the recent years. The 2013 Contest involves two datasets, a hyperspectral image and a LiDAR derived Digital Surface Model (DSM), both at the same spatial resolution (2.5 m). The datasets were acquired over the

Image and Signal Processing for Remote Sensing XX, edited by Lorenzo Bruzzone,
Proc. of SPIE Vol. 9244, 92440P · © 2014 SPIE · CCC code: 0277-786X/14/$18
doi: 10.1117/12.2066616

University of Houston's campus and its neighboring urban area, Huston, Texas, USA [8]. In this paper, we use this hyperspectral image for investigating the capability of hyperspectral data for land cover classification in urban areas.

Figure 1 shows the study area including the University of Houston's campus and the neighboring area. The airborne hyperspectral image was acquired on June 23, 2012 between the times 17:37:10 to 17:39:50 (UTC), by the NSF-funded Center for Airborne Laser Mapping (NCALM). Note that the local standard time in Texas is UTC -6 hours, and thus the image was taken about 20 - 23 minutes before noon. CASI-1500 visible to near-infrared (VNIR) hyperspectral sensor [9, 10] was used for the aerial observation and the acquired image consists of 144 spectral bands (up to 288 bands) in the 380 nm to 1050 nm region, that has been calibrated to at-sensor spectral radiance units [8]. The average height of the sensor above ground was about 5,500 ft (1,676 m).

A multispectral image acquired by WorldView-2 (WV2) satellite on October 16, 2010 at 17:27:02 (UTC) was also introduced in this study (**Figure 1**) for the purpose of comparing with the hyperspectral image. The WV2 imagery consists of a Panchromatic band (0.5 m resolution) and 8 multispectral (2.0 m resolution) in the 425 nm to 950 nm region. Considering the difference of spatial resolutions between the hyperspectral and multispectral datasets, pansharpening was not applied to the WV2 data. **Figure 2** compares these two imagery data for the CASI-1500 imaging area. Because of the cloud cover seen in the hyperspectral image, the area with the red square was selected for a detailed investigation. These true color plots were made by selecting each band (B, G, R) having the highest value at WorldView-2's relative response ([11] shown in **Figure 3**) for the hyperspectral data and B (band-2), G (band-3), and R (band-4) for the multispectral image.

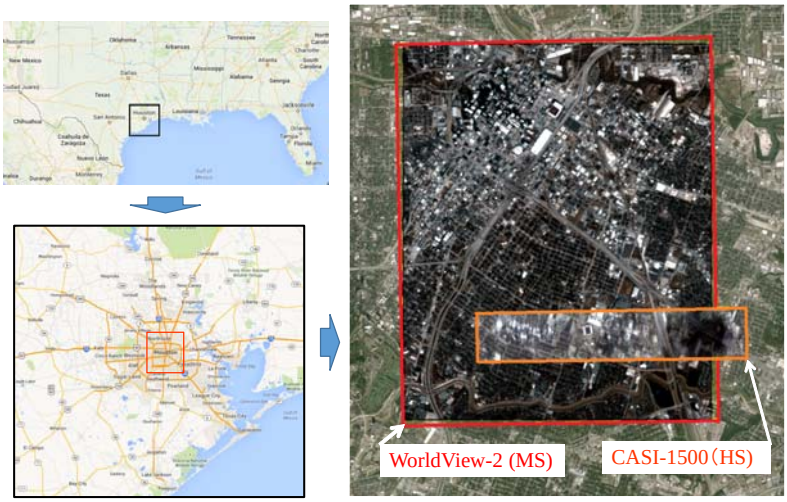

Figure 1. The study area including the University of Houston's campus and the neighboring urban area in Houston, Texas, USA and imaging areas of hyperspectral and multispectral data.

Figure 2. True color composites of the hyperspectral image (top) and the multispectral image (bottom) for the CASI-1500 imaging area. The red square shows the study area.

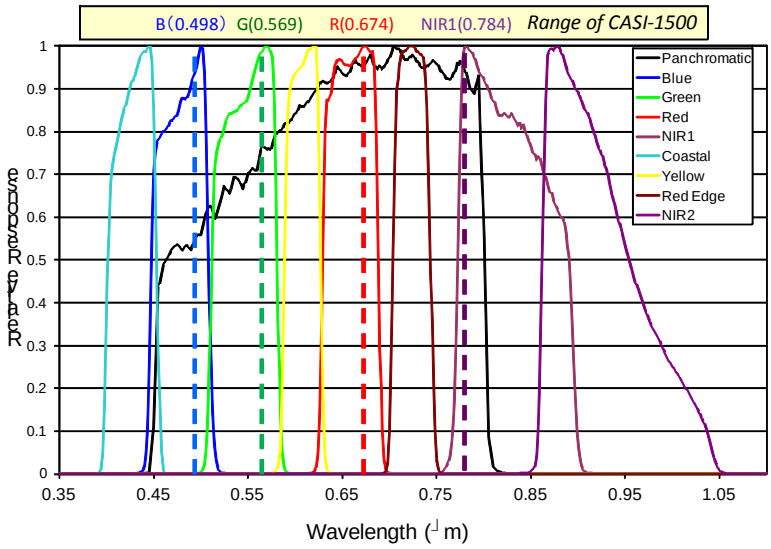

Figure 3. The relative spectral radiance response for WorldView-2 sensors [11] and the range of CASI-1500 hyperspectral sensor

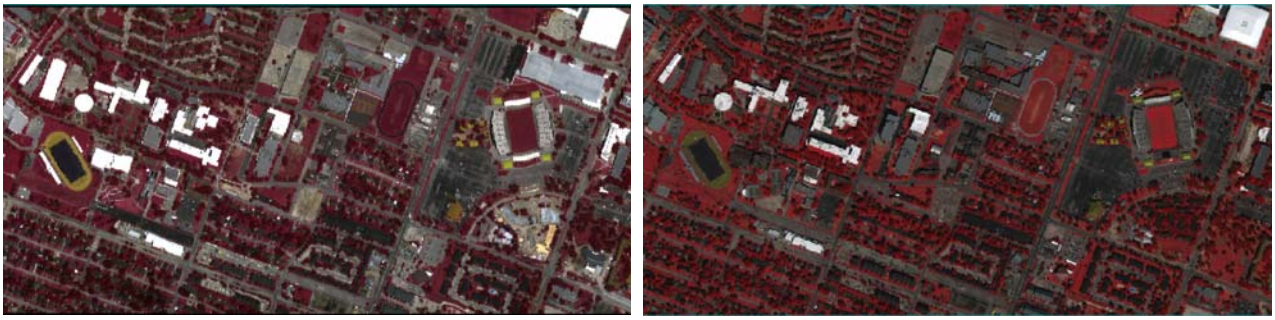

Figure 4. False color composites from the hyperspectral image (left) and multispectral image (right) corresponding to the red square in Figure 2

False color composite images (**Figure 4**) were also produced for the multispectral image (B: band-3, G: band-4, R: band-7) and for the hyperspectral image of the corresponding nearest bands (dotted lines in **Figure 3**). The false color composites showed that a lot of vegetation, seen in red color, exists in the case study site.

3. FIELD SURVEY AND SPECTRORADIOMETER OBSERVATION

In order to obtain ground truth data on spectroradiometric characteristics of surface materials in the study area, a field survey was conducted by the present authors on August 6th and 7th, 2013. A hand-held MS-720 spectroradiometer [12] made by EKO Instruments Co., Ltd., Japan was used. We have used this instrument for several years, e.g. to measure the health condition of tsunami-affected vegetation [13] and the irradiance of sunlit and shadowed Earth surfaces [14].

Figure 5 shows the study area including Texas Southern University's football stadium (**a-d**), University of Houston' campus (**e**) and surroundings together with the locations and photos of six spectroradiometer observation points. The measurements were carried out in the times 15:45 to 16:45 (the local standard time: UTC -6) on August 6 and 10:00 to 10:40 on August 7, 2013. The weather was basically sunny but sometimes cloudy. We measured the irradiances of several surface materials in the study area and that of a white ceramic plate for reference. It is by no means easy to collect field data on the same time and date of spaceborne or airborne data acquisition. So we conducted the survey on

the occasion of our trip to the USA, but the data we collected were almost in the same season (summer) with the hyperspectral image acquisition.

Figure 6 shows the reflectance for six surface materials (lawn, artificial turf, concrete, soil, link-stone, asphalt) from the hyperspectral (HS) image and by our spectroradiometer field measurement. The pseudo-reflectance for the HS image

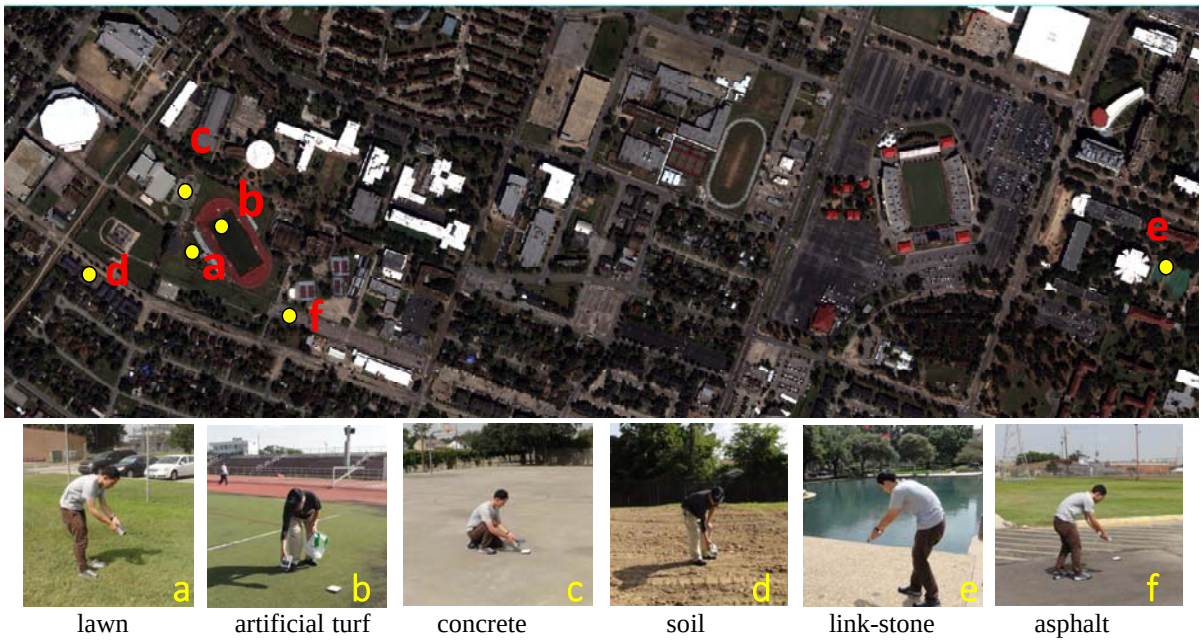

Figure 5.The study area including Texas Southern University's football stadium (**a-d**), University of Houston' campus (**e**) and surroundings together with the locations and photos of six spectroradiometer observation points.

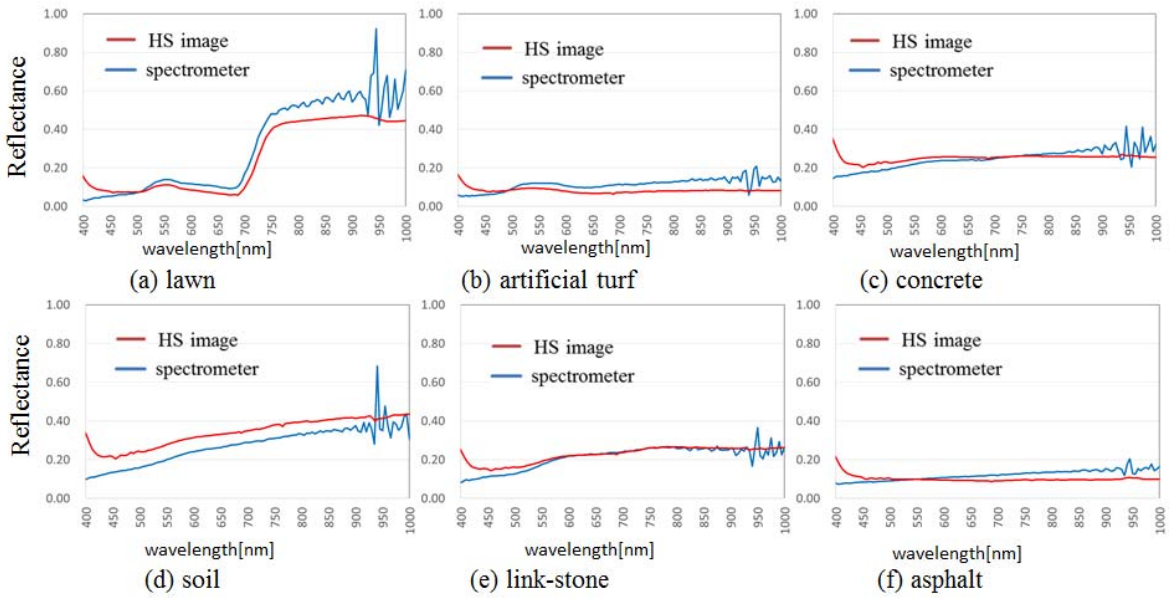

Figure 6. Reflectance for six surface materials (lawn, artificial turf, concrete, soil, link-stone, asphalt) from the hyperspectral (HS) image and by our spectroradiometer field measurement.

was obtained by dividing the 144 digital numbers (DN) corresponding to the HS bands at each pixel by those of the brightest pixel (a white roof in the image). The reflectance values by the field measurement were obtained as the spectral ratio between a surface material and the white plate measured at the same time instant. Although some fluctuations are seen in the shorter wavelength range (for the HS image) and in the longer wavelength range (for the spectrometer), the obtained spectral reflectance curves for the six materials are quite similar. Since the reflectance is unique to surface materials and basically do not depends on the sunlight condition, the result is reasonable and convincing.

4. PRINCIPAL COMPONENT ANALYSIS

Comparison of the hyperspectral (HS: CASI-1500) and multispectral (MS: WV-2) data was carried out with the aid of a Principal Component Analysis (PCA). **Figure 7** compares the intensity images for the first, second and third principal components (PC) for the MS and HS imagery. The PC-1 images for the MS and HS corresponded to the brightness (intensity) value, and thus white roofs of buildings showed higher values in them. One the contrary, the large values in the PC-2 images corresponded to vegetation. This fact could be confirmed by comparing the PC-2 value and the NDVI

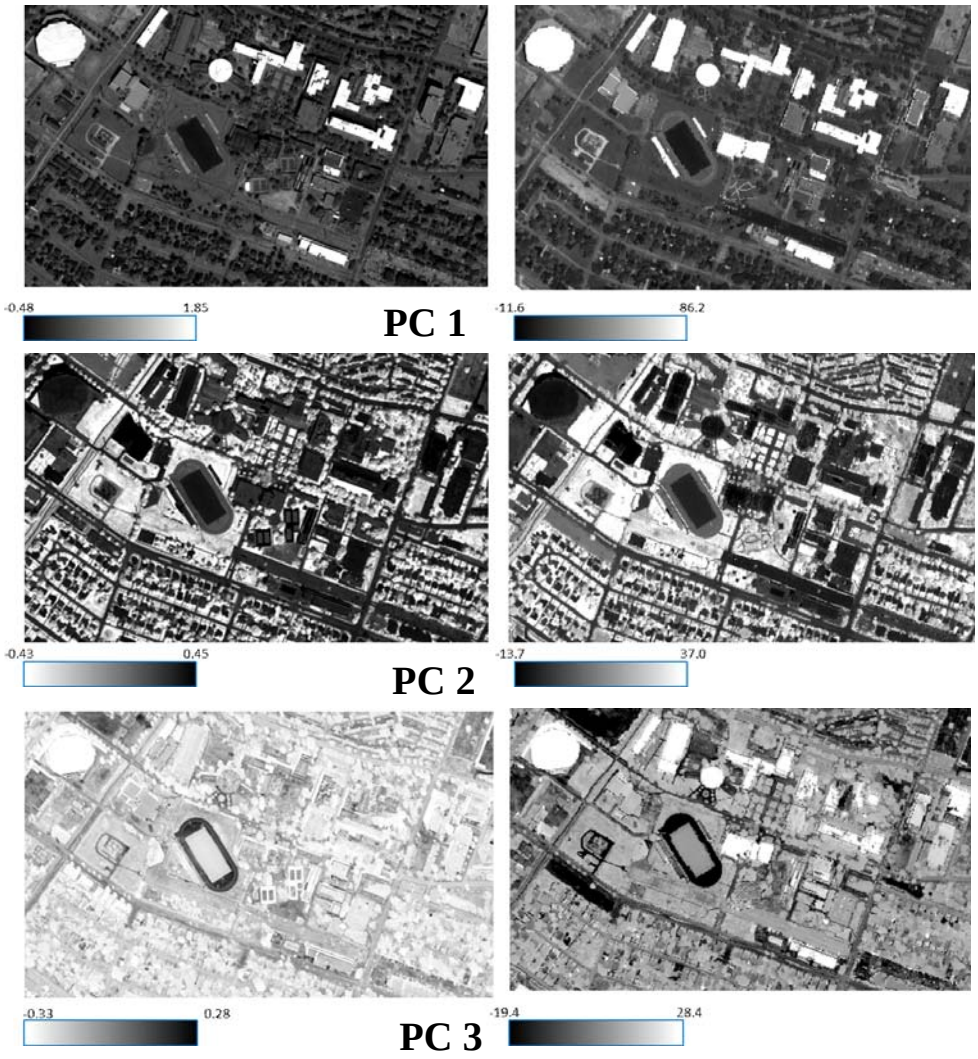

(a) WorldView-2 (MS) image (b) Hyperspectral (HS) image

Figure 7. Comparison of intensity images for the first, second and third principal components (PC)

value (Red: bands 53-73, NIR: bands 80-144) in **Figure 8**, in which higher values (red color in the rainbow color plot) are observed in vegetation. A similar correspondence with the PC-2 and NDVI values was also observed for the MS image. A clear relationship with surface materials is not seen for the PC-3 value in **Figure 7**.

Figure 9 shows the cumulative ratio of the variances in the PCA for the MS and HS images. Although there are 8 bands in the MS image, the cumulative variance ratio reached 0.840 by the PC-1, and 0.989 until the PC-2. Thus it was concluded that the brightness and vegetation are the dominant factors for the digital numbers (DNs) of the MS image. For the HS image, the cumulative variance ratio reached 0.662 by the PC-1, and 0.983 until the PC-2, and thus the PC-1 and 2 can represent almost all the information included in the HS image. This means that although there are 144 bands in the HS image, only the first and second principal components are meaningful. This observation could also be confirmed from **Figure 6**, in which the spectral signatures for the manmade objects are almost flat, representing only the brightness value controls the spectral characteristics. Thus it is concluded that other than the case of detailed classification for vegetation, hyperspectral imagery is not so effective for land-cover classification of urban areas.

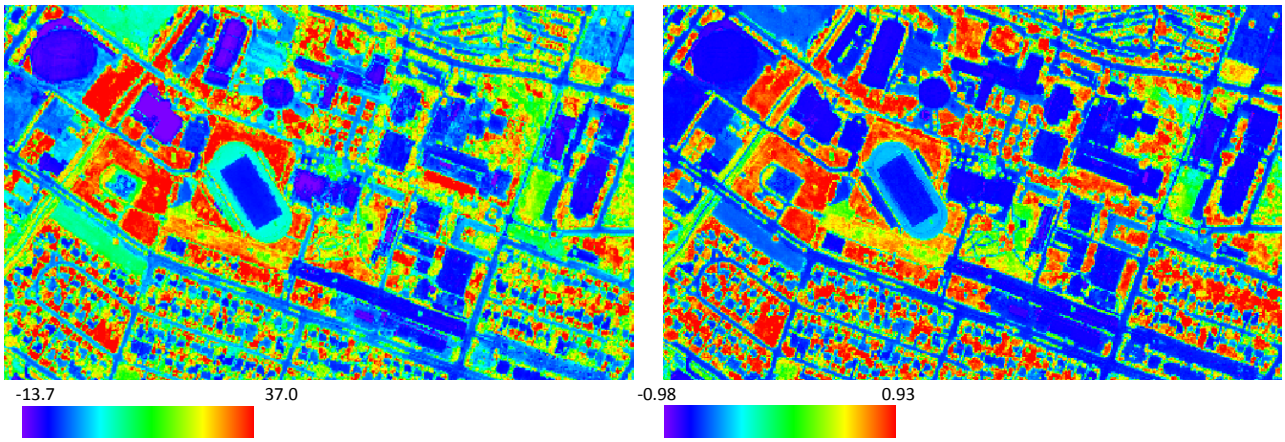

(a) PC-2 image (b) NDVI value where (Red: bands 53-73, NIR: bands 80-144)

Figure 8. Comparison of the PC-2 and NDVI values for the hyperspectral (HS) image

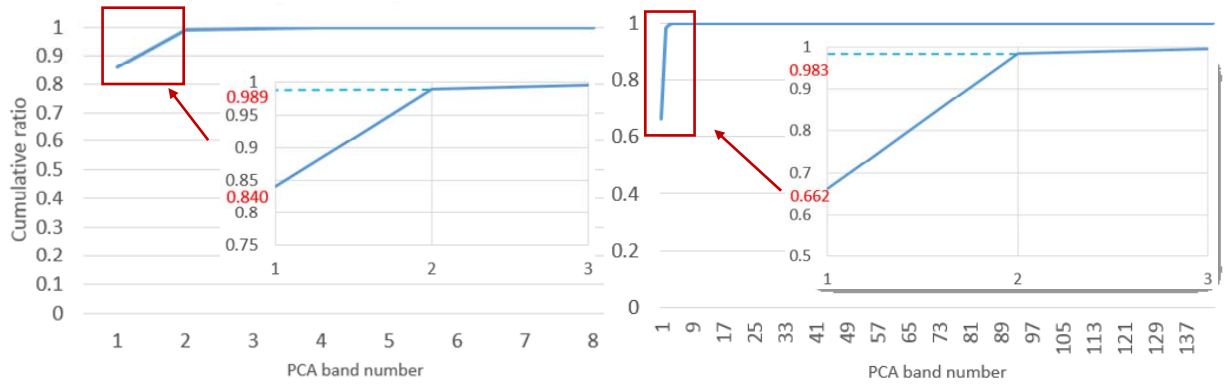

(a) WorldView-2 (MS) image (b) Hyperspectral (HS) image

Figure 9. Cumulative ratio of the variances in the PCA for the MS and HS images.

5. CONCLUSIONS

Using the airborne hyperspectral (HS) data acquired by CASI-1500 imager over Houston, Texas, USA, the spectral reflectance characteristics of surface materials were investigated. The HS data include 144 spectral bands in the visible to near-infrared (380 nm to 1050 nm) regions. A multispectral (MS) image acquired by WorldView-2 satellite was

introduced in order to compare it with the HS image. A field measurement was also carried out using a handheld spectroradiometer by the authors. The reflectance of surface materials obtained by the measurement was compared with the pseudo-reflectance of the HS data and they showed good agreement. Finally a principal component analysis was conducted for the HS and MS data and the result showed that the HS imagery is not so useful for the classification of land-cover in urban areas.

ACKNOWLEDGMENT

The hyperspectral data used in this study were provided from the 2013 IEEE Geoscience and Remote Sensing Society Data Fusion Contest.

REFERENCES

[1] Rathje, E., and Adams, B.J., "The role of remote sensing in earthquake science and engineering, opportunities and challenges," *Earthquake Spectra*, 24(2), 471–492 (2008).

[2] Eguchi, R.T., Huyck, C., Ghosh, S., Adams, B.J., "The application of remote sensing technologies for disaster management," *The 14th World Conference on Earthquake Engineering*, CD-ROM, 17p (2008).

[3] Brunner, D., Lemoine, G., and Bruzzone, L., "Earthquake damage assessment of buildings using VHR optical and SAR imagery," *IEEE Transactions on Geoscience and Remote Sensing*, 48(5), 2403-2420 (2010).

[4] Meslem, A., Yamazaki, F., Maruyama, Y., "Accurate evaluation of building damage in the 2003 Boumerdes, Algeria earthquake from QuickBird satellite images," *Journal of Earthquake and Tsunami*, 5(1), 1-18 (2011).

[5] Bioucas-Dias, J.M., Plaza, A., Camps-Valls, G., Scheunders, P., Nasrabadi, N.M., Chanussot, J., "Hyperspectral remote sensing data analysis and future challenges," *IEEE Geoscience and Remote Sensing Magazine*, 1(2), 6-36 (2013).

[6] MicroImages, Inc., Introduction to hyperspecral imaging, (2012). Available online: http://www.microimages.com/documentation/Tutorials/hyprspec.pdf (accessed on 14th September 2013).

[7] Pompilio, L., Villa, P., Boschetti, M., Pepe, M., "Spectroradiometric field surveys in remote sensing practice: a workflow proposal, from planning to analysis," *IEEE Geoscience and Remote Sensing Magazine*, 1(2), 37-51 (2013).

[8] 2013 IEEE GRSS Data Fusion Contest, Fusion of Hyperspectral and LiDAR Data (2013). Available online: http://www.grss-ieee.org/community/technical-committees/data-fusion/data-fusion-contest/ (accessed on 14th September 2013).

[9] ITRES Research Limited, CASI-1500 Hyperspectral Imager (2011). Available online: http://www.itres.com/products/imagers/casi1500/ (accessed on 14th September 2013).

[10] ITRES Research Limited, Operations and Mission Planning for ITRES' CASI 1500h system (2006). Available online: ftp://snr-0563.unl.edu/Incoming/For_Rick/CASItraining/CASI_1500h_System_Op_Training.ppt (accessed on 14th September 2013).

[11] DigitalGlobe, Inc., Radiometric Use of WorldView-2 Imagery: Technical Note (2010). Available online:http://www.digitalglobe.com/sites/default/files/Radiometric_Use_of_WorldView-2_Imagery%20(1).pdf (accessed on 14th September 2013).

[12] EKO Instruments Co., MS-720 Spectroradiometer (2013). Available online: http://eko-eu.com/products/solar-radiation-and-photonic-sensors/spectroradiometers/ms-720-spectroradiometer (accessed on 14th September 2013).

[13] Yamazaki, F., Matsuoka, M., Warnitchai, P., Polngam, S., Ghosh, S., "Tsunami Reconnaissance Survey in Thailand Using Satellite Images and GPS," *Asian Journal of Geoinformatics*, 5(2), 53-61 (2005).

[14] Liu, W., Yamazaki, F., "Object-based shadow extraction and correction of high-resolution optical satellite images," *IEEE Journal of Selected Topics in Applied Earth Observations and Remote Sensing*, DOI: 10.1109/JSTARS.2012.2189558, 5(4), 1296-1302 (2012).